Breaking Capability of a SF6 Circuit Breaker for Short Circuits Close to a Generation Unit with Delayed Current Zero Crossing

M. Kizilcay

Abstract-- **Depending on the instant and type of short circuit, and pre-fault operation state of the synchronous generator, the short circuit current may have delayed zero crossing in case of short circuits close to a generation unit. The switching arc drawn between the circuit breaker contacts causes a faster attenuation of the DC component, thus zero crossing of the SC current may occur sooner.**

In this paper the breaking capability of a 170-kV circuit breaker for a generator unit will be analyzed under worst-case conditions, which is connected to a 154-kV grid. The influence of the instant of the short circuit begin, CB arc model parameters and fault arc on current interruption is shown by means of ATP-EMTP simulations.

Keywords: **circuit breaker, synchronous generator, breaking capability, delayed current zero crossing, circuit breaker arc, EMTP.**

I. INTRODUCTION

When a short-circuit close to a synchronous generator occurs, depending on the instant of short circuit (SC) begin and under-excited state of pre-fault operation, the transient DC component of the fault current may exceed the AC component and/or the subtransient AC component may decay faster than the DC component, resulting in short-circuit current not crossing zero for several cycles. This is termed a delayed current zero crossing phenomenon, which can impose great problem on an AC circuit breaker (CB). A number of studies [1] - [3] have been reported that have analyzed the interrupting phenomenon in a power transmission system through computer simulation.

The switching arc drawn between the circuit breaker contacts during interruption causes a rapid attenuation of the DC component, thus zero crossing of the SC current occurs sooner.

In this paper the breaking capability of a 170-kV SF$_6$ circuit breaker for a hydropower synchronous generator unit will be analyzed under worst-case conditions. Interruption of a metallic short circuit behind the unit transformer of a 97-MVA synchronous generator will be investigated under different pre-fault operation modes, whereas the current interruption by

the CB will be computed using a generalized arc model [4], [6]. EMTP-ATP is used for the numerical simulations [6]. Influence of the CB arc model parameters, instant of the short circuit begin and type and fault arc on current interruption will be shown.

II. FACTORS EFFECTING SHORT CIRCUIT CURRENT WAVEFORM

A. Pre-Fault Operation of the Generator

The worst-case regarding the delay of current zero crossing is expected, when a two-phase short circuit turns into a three-phase circuit circuit with a delay of ¼ period (5 ms for $f = 50\,\text{Hz}$) under a pre-fault operation of the generator in the under-excited state (leading current) [1], [2]. A metallic fault (negligible fault resistance) is assumed at the 154-kV grid side of the CB. Additionally, a simultaneous three-phase short circuit during an under-excited operation is studied.

Other less critical pre-fault operation modes of the generator investigated are:
- running at no-load ($P_{gen} = 0\,\text{MW}; Q_{gen} = 0\,\text{Mvar}$)
- over-excitation of the generator at rated power, ($P_{gen} = 87.3\,\text{MW}; Q_{gen} = 42.3\,\text{Mvar}$)

B. Instant of Fault Occurrence

The instant of fault inception influences the amplitude of the DC component of the SC current. The worst-case is expected, if a two-phase fault occurs at zero-crossing of the phase-to-phase voltage, $u_{ab} = 0$, which progresses to a three-phase fault after ¼ period (5 ms) [1], [3]. In case of simultaneous three-phase fault, initiation of the fault at zero-crossing of the phase a voltage, $u_a = 0$, causes maximum DC current component in phase a. In contrary, initiation of the fault at voltage peak of phase a (equivalent to zero-crossing of phase-to-phase voltage between b and c), causes larger DC components in the currents of phase b and c.

III. SYSTEM DATA AND REPRESENTATION

A. Synchronous Generator

The data of the synchronous generator are summarized in Table 1. The generator is modelled using type-59 dynamic synchronous machine component of EMTP-ATP. The electrical part is described by Park equations in *d-q-0* components. The simple single-mass representation is applied

Mustafa Kizilcay is with the University of Siegen, Department of Electrical and Computer Engineering, Siegen, Germany (e-mail: kizilcay@ieee.org).

for the mechanical part, which is adequate for hydro units and for the concerning short circuit duration. In fact the precise representation of the mechanical part of the generator and turbine is not necessary for the computation of SC currents.

parameter	value	parameter	value
S_r	97 MVA	x_q	0.65 pu
U_r	13.8 kV	x_q'	0.65 pu [1]
pole pairs	14	x_q''	0.192 pu
x_d	1.10 pu	T_q'	0 [1]
x_d'	0.282 pu	T_q''	0.064 s
x_d''	0.214 pu	r_a	0.0025 pu
T_d'	2.69 s	x_l	0.16 pu [2]
T_d''	0.063 s	J	1.2·10⁶ kg·m² [2]

[1] $x_q' = x_q$ and $T_q' = 0$ imply absence of the g-winding (eddy-current winding) on the quadrature axis of the type-59 synchronous machine model
[2] assumed values taken from [7] for a hydro unit with rated power of 100 MVA

B. Generator Bus Duct

The high-current generator bus duct is represented by its total resistance

$$R_{total} = R_{dc}' \cdot l = 5.32\,\mu\Omega/m \cdot 31.1\,m = 165.45\,\mu\Omega,$$

which is relatively small. The inductance of the bus duct is neglected compared to the series connected generator and transformer inductance.

C. Unit Transformer

The unit transformer is modelled as a three-phase, 3-leg transformer in ATPDraw [8] using *Hybrid Model* based on the data given in Table 2. The transformer is represented as a linear component, i.e. the saturation of the iron core does not need to be considered, because only the short circuit behaviour has been analyzed.

TABLE 2
ELECTRICAL DATA OF THE UNIT TRANSFORMER

rated power	97 MVA
medium tap voltage ratio (HV/LV)	154 kV / 13.8 kV
percent impedance voltage at medium tap	12.5 %
load losses at rated current	312 kW
no load losses at rated voltage	57 kW
magnetizing current	0.2 % of I_r

D. Short 154-kV Overhead Line

The unit transformers are connected to the outdoor switchyard by relatively short overhead lines (OHL) via one tower. The conductor type is ACSR 405/52 "Condor". The shortest line length is 27.2 m for unit 3 and the longest one (unit 1) amounts to 80 m. As worst-case the shortest line length is used for the simulations in section 4. Electrical data of the OHL are calculated by LINE CONSTANTS routine [6] as follows:
- positive-sequence:
$$\underline{Z}_{(1)} = (0.0724 + j0.3625)\ \Omega/km;\quad C_{(1)} = 10.09\ nF/km$$
- zero-sequence:
$$\underline{Z}_{(0)} = (0.21628 + j1.413)\ \Omega/km;\quad C_{(0)} = 4.89\ nF/km.$$

E. 154-kV Network Equivalent

The 154-kV network is represented at the 154-kV busbar by a Thevenin equivalent consisting of the short circuit impedance and voltage source. The initial symmetrical short circuit power is given as $S_k'' = 3118\,MVA$ including the three hydro-electric power units. The X/R-ratio of the SC impedance is given as 13.68. The positive-sequence SC impedance of the 154-kV equivalent network seen from one generator amounts to $\underline{Z}_{(1)sc} = (0.71 + j9.72)\ \Omega$. The zero-sequence SC impedance at the 154-kV busbar is estimated using known short-circuit powers for three-phase and single-phase short circuits. The ratio of the zero to positive sequence impedance is $\dfrac{Z_{(0)sc}}{Z_{(1)sc}} = 2.68$.

F. Circuit Breaker

The 170-kV SF6 generator circuit breaker is located at the HV side of the unit transformer. The relay time is specified as 10 ms, whereas opening time of the CB is 29 ms. Thereafter the arcing time begins. Hence the current interruption starts 39 ms after the fault initiation. A dynamic arc model [4], [5] is used to represent the CB during the arcing period. The model consists of the combination of Mayr and Cassie models. The series connection of the time-varying arc resistances computed by solving the arc equations with constant parameters according Mayr and Cassie is used to represent the CB arc. The Mayr and Cassie differential equations are expressed as generalized arc equation [9]

$$\frac{dg}{dt} = \frac{1}{\tau}(G - g) \tag{1}$$

where τ : is the arc time constant, standing for τ_m, τ_c
g : instantaneous arc conductance,
G : stationary arc conductance.

The stationary arc conductance G_m is defined for the Mayr equation as:

$$G_m = \frac{i_{arc}^2}{P_0} \tag{2}$$

where P_0 : steady-state heat dissipation

The stationary arc conductance G_c for the Cassie equation:

$$G_c = \frac{|i_{arc}|}{u_0} \tag{3}$$

where u_0 : constant arc voltage valid at high currents.

The Mayr equation describes the arc behaviour in the region close to the current zero passing. The decision for arc extinction is made dominantly by the Mayr equation. The Cassie equation describes the arc accurately for high currents. The total arc conductance is calculated using (4):

$$\frac{1}{g} = \frac{1}{g_m} + \frac{1}{g_c} \tag{4}$$

g_m and g_c are arc conductance of Mayr and Cassie models, respectively.

The arc equations are described and solved in MODELS simulation language. The arc is represented by type-91 time-varying resistance in EMTP-ATP.

The only parameter that is known for that CB is the minimum arc voltage $u_0 = 500\,\mathrm{V}$. Remaining values are taken from [4] given for a 110-kV SF$_6$ CB:

$$P_0 = 8800\,\mathrm{W}; \quad \tau_m = 0.22\,\mu\mathrm{s}; \quad \tau_c = 0.8\,\mu\mathrm{s}$$

IV. COMPUTATION RESULTS

In the following sections the simulation results will be presented for the worst-case of pre-fault operation modes of the synchronous generator with different fault inception instants. Fig. 1 shows the single-line diagram of the 97-MVA hydro-electric generation unit modelled using ATPDraw. The capability diagram of the generator given in Fig. 2 is used to select different pre-fault operation states. The pre-fault operating points used for the simulations are given in Table 3 and indicated also in Fig. 2.
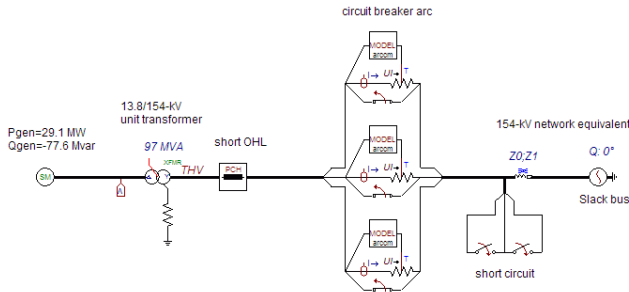

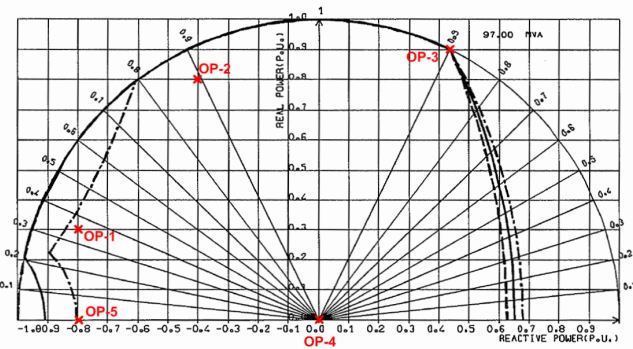Fig. 1. Single-line diagram of the circuit with 97-MVA generation unit

Fig. 2. Capability diagram of the hydro-electric generator

For each pre-fault operating point of the generator, four different fault inception instants shown in Table 4 have been defined referring to [2]. The simulation cases will be named according to Tables 3 and 4. For example, OP-1C means a non-simultaneous fault (transition from two-phase to three-phase fault) for the under-excited generation according to pre-fault operation point OP-1. All pre-fault conditions have been determined by the load flow (FIX SOURCE) option of the EMTP-ATP automatically as steady-state condition [6].

TABLE 3
STUDIED PRE-FAULT OPERATING POINTS OF THE GENERATOR (S_{BASE} = 97 MVA)

Pre-fault operating point	P in pu / MW	Q in pu / Mvar
OP-1 (under-excitation)	0.3 pu / 29.1 MW	−0.8 pu / 77.6 Mvar
OP-2 (under-excitation)	0.8 pu / 77.6 MW	−0.4 pu / 38.8 Mvar
OP-3 (over-excitation at rated operating point)	0.9 pu / 87.3 MW	0.436 pu / 42.3 Mvar
OP-4 (no-load)	≈ 0	≈ 0
OP-5 (reactive power only)	≈ 0	−0.8 pu / 77.6 Mvar

TABLE 4
INSTANTS OF FAULT OCCURRENCE

Case ID	Fault type *	Description
A	k3	simultaneous three-phase fault at zero-crossing of u_A
B	k3	simultaneous three-phase fault at peak value of u_A
C	k2 → k3	non-simultaneous fault: two-phase fault at zero-crossing of u_{AB} and transition to a three-phase fault after 5 ms ($u_C = 0$)
D	k2E → k3E	non-simultaneous fault: two-phase earth fault at zero-crossing of u_{AB} and transition to a three-phase earth fault after 5 ms ($u_C = 0$)

* fault type symbols according to IEC 909

It is assumed that the fault type given in Table 4 occurs right behind the concerning 170-kV circuit breaker without any fault resistance (worst-case). Any arc in air at fault location would significantly increase the resistance of the fault path impedance and decrease the time constant of the DC component of the short circuit current. In the following the worst-case of pre-fault operation OP-1 of the generator (under-excited operation) according to Table 3 will be presented, which causes the maximum arcing time in the CB.

A. Short Circuit in Under-excited State at Operation Point OP-1

The maximum arcing time of 159 ms in the CB is expected for a non-simultaneous short circuit, case OP-1C. The arcing time should be in general shorter than 15 ms for the power frequency of 50 Hz.

The computation results of the case OP-1C are shown in Fig. 3 and Fig. 4. In Fig. 4 the fault is initiated at $t_1 = 3.3$ ms. Contact separation (t_2) takes place 39 ms after the fault occurrence (t_1). Phase a current is interrupted at its next zero-crossing within a few ms. Maximum arcing time 159 ms ($= t_3 - t_2$) is expected in phase b because of missing current zeros.
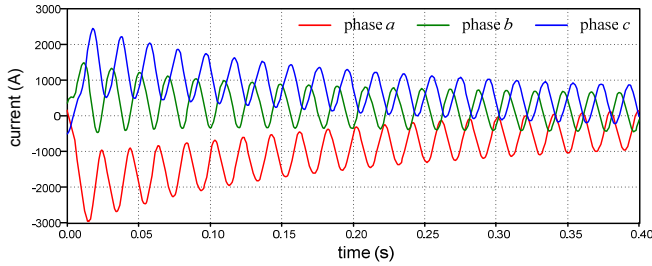
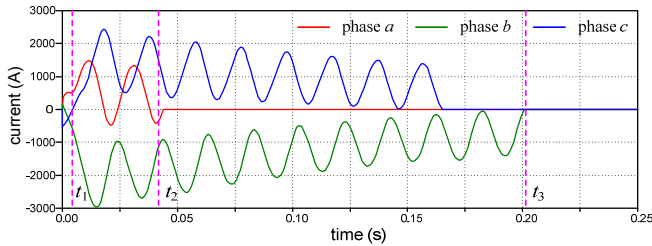Fig. 3. Prospective 3-phase short circuit current (no CB arc). Case OP-1C

Fig. 4. Interruption of the non-simultaneous 3-phase short circuit current by CB Case OP-1C (arcing time = 159 ms)

B. Influence of Circuit Breaker Arc Parameters on the Delay of Current Zero Crossing

In [5] the arc voltage for the Cassie model is determined for a 110-kV SF_6 circuit breaker as

$$u_0 = 2350\,\text{V} \, .$$

This value is higher than $u_0 = 500\,\text{V}$ given for the 170-kV circuit breaker. In order to see the influence of the arc voltage u_0 on arcing time, simulations are repeated for the values:

$$u_0 = 1000\,\text{V} \quad \text{and} \quad u_0 = 2000\,\text{V} \, .$$

Other arc parameters P_0, τ_m and τ_c are kept unchanged. The simulations results for the case OP-1C (compare to Fig. 4) are shown in figures 5 and 6.
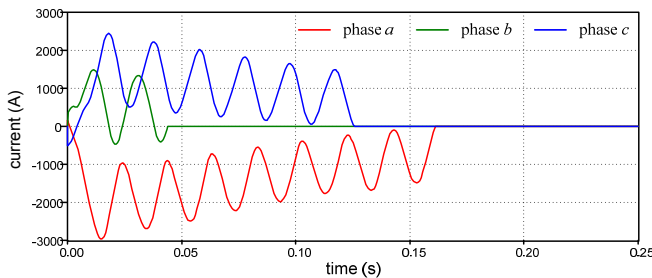

Fig. 5. Interruption of the non-simultaneous 3-phase short circuit current by CB, Case OP-1C. $u_0 = 1000\,\text{V}$ (arcing time = 119 ms)
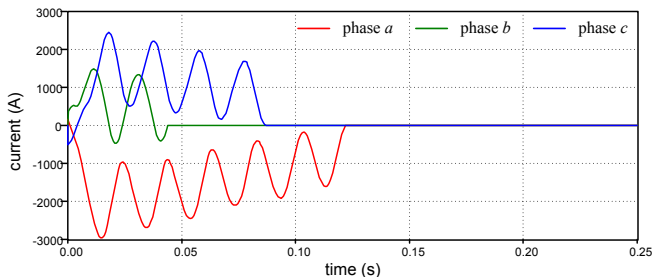

Fig. 6. Interruption of the non-simultaneous 3-phase short circuit current by CB, Case OP-1C. $u_0 = 2000\,\text{V}$ (arcing time = 80 ms)
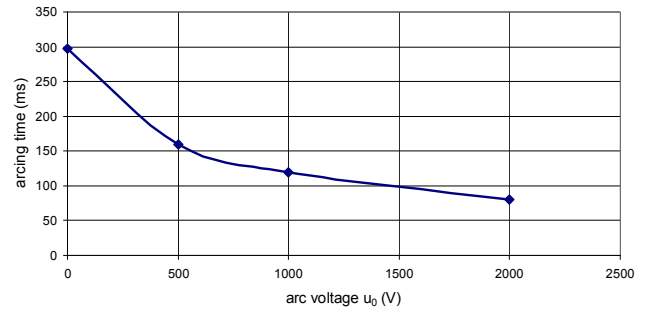

Fig. 7. Variation of arcing time depending on the arc voltage u_0

The relation between the arcing time and arc voltage u_0 is given in Fig. 7.

C. Influence of the Fault Arc on the Short Circuit Current Waveform

It is known that the fault arc in air may significantly decrease the time constant of the DC component of the short circuit current. For comparison purpose the non-simultaneous short circuits under under-excited pre-fault load condition of the generator are computed by taking into account the fault arc as a dynamic component in the simulation model [10], [11]. Case OP-1C with a non-simultaneous short circuit (transition from two-phase to three-phase arc fault without earth connection) and longest arcing time 159 ms is selected for comparison. The fault arc length is set equal to the distance between phase conductors, which is 2.9 m. Arc elongation is not taken into account. The arc parameters used to simulate the fault arcs are

$$u_0' = 1.04\ \text{kV/m}; \quad r_0' = 40\ \text{m}\Omega/\text{km}; \quad \tau_0 = 1\ \text{ms}.$$

The CB arc with $u_0 = 500\,\text{V}$ as well as the fault arc are considered in the simulation of case OP-1C. The SC current in each phase is compared in Fig. 7 with the results given in Fig. 4. It can be seen that the delay of missing zero crossing of the SC currents becomes significantly shorter due to the non-linear fault arc resistance, which decreases the time constant of the DC component of the SC current.
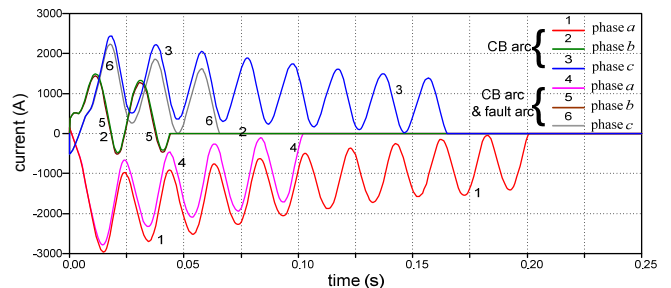

Fig. 7. Comparison of the SC currents for the case OP-1C; Simulation of the current interruption with CB arc versus simulation with CB and fault arc

D. Measure Against Long Arcing Time

It will be necessary to delay the opening of the circuit breaker by the protection taking into consideration the worst-case, if applicable, in order to decrease the arcing time to

maximum 20 ms, i.e. one period. For this purpose the maximum SC current zero crossing delay is to be specified by analyzing the delay of the zero crossing of the prospective SC current without influence by the CB arc for the cases defined in Tables 3 and 4. Case OP1-D, i.e. non-simultaneous fault, when a two-phase fault evolves into a three-phase fault, during under-excited operation of the generator, results in the maximum time delay, $t_{\text{zero-delay}} = 399$ ms for the SC current zero crossing. Considering a maximum allowed arcing time of the CB of one period, i.e. 20 ms, relay time, $t_{\text{relay}} = 10$ ms , and opening time, $t_{\text{open}} = 29$ ms , of the CB (after this time delay arcing in CB starts), the relay "off" signal must be delayed $t_{\text{off-delay}} = 340$ ms for the worst case, OP1-D, using the equation

$$t_{\text{off-delay}} = t_{\text{zero-delay}} - t_{\text{relay}} - t_{\text{open}} \qquad (5)$$

The SC current interruption for the case OP-1D with the "off" signal delay 340 ms by the relay is shown in Fig. 8. The CB arc in the simulation model is after $t_{\text{off-delay}}$ active.
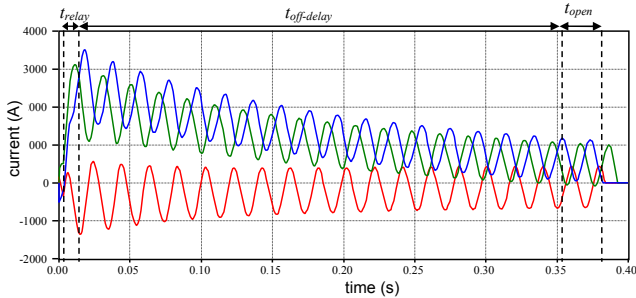

Fig. 8. Interruption of the non-simultaneous 3-phase short circuit current by the CB arc. Case OP-1D with relay "off" signal delay 340 ms (arcing time = 14 ms)

V. CONCLUSION

The breaking capability of a 170-kV SF_6 circuit breaker for a hydro-electric generation unit has been studied for short circuits in a 154-kV grid close to the generation unit. Particularly, the delay of zero crossing of CB pole currents has been analyzed because this phenomenon may cause high stress on CB. The pre-fault operation state of the synchronous generator plays an important role regarding delayed zero crossing of the short circuit current due to the DC component of the SC current. Under-excited operation state is unfavourable in this respect. The amplitude of the DC component is also affected by the instant of fault inception. As worst-case a metallic fault without arc is taken into account in the computations.

Out of five pre-fault operation points of the generator investigated, the under-excited operation (case OP-1) results for a non-simultaneous short circuit (transition from a two-phase to a three-phase fault) in the maximum arcing time of 159 ms, when the relay "off" signal is not delayed. The short circuit is assumed to occur in the 154-kV switchyard behind the circuit breaker as worst-case.

Another case studied but not presented in the paper is a short circuit between unit transformer and circuit breaker in the short 154-kV overhead line. In this case short circuit currents from the other two generation units of the hydropower plant and the short circuit current from the 154-kV grid will superpose and flow through the circuit breaker. Due to high short circuit current injected from the 154-kV grid, no missing zero crossing in the CB current occurs even under the unfavourable pre-fault operation of the generators. Consequently this fault case is not critical regarding CB operation.

It will be necessary to delay the opening of the circuit breaker 340 ms by the protection for the worst-case, if applicable, in order to decrease the arcing time to maximum 20 ms, i.e. one period.

When instead of a metallic fault an arc fault in air occurs, then the delay of zero crossing of the short circuit current will be substantially reduced as shown by the numerical simulations.

The computation results with the consideration of the CB arc and fault arc models may contain uncertainty because no measurement could be made using the real CB. They should be seen however as indication.

VI. REFERENCES

[1] B. Kulicke, H.-H. Schramm, "Clearance of Short-Circuits with Delayed Current Zeros in the Itaipu 550kV-Substation", *IEEE Transactions on Power Apparatus and Systems*, Vol. PAS-99, pp. 1406-1414, July/Aug. 1980.

[2] R. Brinkhoff, B. Kulicke, H.-H. Schramm, "Ausschalten nicht-simultaner Kurzschlüsse mit ausbleibenden Stromnulldurchgängen durch SF6-Blaskolbenschalter (title in English: Clearance of non-simultaneous short circuits with delayed current zero crossings by a SF6 puffer circuit breaker)", *Elektrizitätswirtschaft*, Vol. 77, No. 11, pp. 385-393, 1978.

[3] M. Ishikawa, H. Ikeda, S. Yanabu, M. Yamamoto, "Numerical Study of Delayed-Zero-Current Interruption Phenomena Using Transient Analysis Model for an Arc in SF6 Flow", *IEEE Transaction on Power Apparatus and Systems*, Vol. PAS-103, No. 12, pp. 3561-3568, December 1984.

[4] U. Habedank, "Application of a New Arc Model for the Evaluation of Short-circuit Breaking Tests", *IEEE Transactions on Power Delivery*, Vol. 8, No. 4, pp. 1921-1925, October 1993.

[5] G. Bizjak, P. Zunko, D. Povh, "Combined Model of SF6 Circuit Breaker for Use in Digital Simulation Programs", *IEEE Transactions On Power Delivery*, Vol. 19, No. 1, pp. 174-180, January 2004.

[6] Canadian/American EMTP User Group: ATP Rule Book, Portland, USA (http://www.emtp.org)

[7] P. M. Anderson, A. A. Fouad, *Power System Control and Stability*, The Iowa State University Press, USA, 1. edition, 1977.

[8] H. K. Høidalen, B. A. Mork, F. Gonzalez, D. Ishchenko, N. Chiesa, "Implementation and verification of the Hybrid Transformer model in ATPDraw", *Proc. International Conference on Power Systems Transients* (IPST'07) Lyon, France, 2007 (available at http://www.ipst.org)

[9] A. Grütz, A. Hochrainer, "Rechnerische Untersuchung von Leistungsschaltern mit Hilfe einer verallgemeinerten Lichtbogentheorie", *etz-a*, vol.92, no.4, pp.185-191, 1971 (in German).

[10] M. Kizilcay, L. Prikler, G. Ban, P. Handl, "Interaction of the Secondary Arc with the Transmission System during Single-Phase Autoreclosure", *Proc. IEEE Bologna Power Tec 2003*, Bologna, Italy, 2003.

[11] M. Kizilcay, P. La Seta, "Digital simulation of fault arcs in medium-voltage distribution networks", *Proc. 15th Power Systems Computation Conference*, Liège, Belgium, 2005.